

Two gaps with one energy scale in cuprate superconductors

Shiping Feng*, Huaisong Zhao, and Zheyu Huang

Department of Physics, Beijing Normal University, Beijing 100875, China

The interplay between the superconducting gap and normal-state pseudogap in cuprate superconductors is studied based on the kinetic energy driven superconducting mechanism. It is shown that the interaction between charge carriers and spins directly from the kinetic energy by exchanging spin excitations in the higher power of the doping concentration induces the normal-state pseudogap state in the particle-hole channel and superconducting state in the particle-particle channel, therefore there is a coexistence of the superconducting gap and normal-state pseudogap in the whole superconducting dome. This normal-state pseudogap is closely related to the quasiparticle coherent weight, and is a necessary ingredient for superconductivity in cuprate superconductors. In particular, both the normal-state pseudogap and superconducting gap are dominated by one energy scale, and they are the result of the strong electron correlation.

PACS numbers: 74.20.Mn, 74.25.Dw, 74.72.Kf

After intensive investigations over more than two decades, it has become clear that the interplay between the superconducting (SC) gap and normal-state pseudogap is one of the most important problems in cuprate superconductors^{2,3}. The parent compounds of cuprate superconductors are believed to belong to a class of materials known as Mott insulators with an antiferromagnetic (AF) long-range order (AFLRO), where a single common feature is the presence of the CuO₂ plane⁴. As the CuO₂ planes are doped with charge carriers, the AF phase subsides and superconductivity emerges⁴, and then the physical properties mainly depend on the extent of doping, and the regimes have been classified into the underdoped, optimally doped, and overdoped, respectively. Experimentally, a large body of experimental data available from a wide variety of measurement techniques have provided rather detailed information on the normal-state pseudogap state and SC-state in cuprate superconductors²⁻¹³, where an agreement has emerged that the normal-state pseudogap state is particularly obvious in the underdoped regime, i.e., the magnitude of the normal-state pseudogap is much larger than that of the SC gap in the underdoped regime, then it smoothly decreases upon increasing the doping. This is why the normal-state properties in the underdoped regime exhibit a number of the anomalous properties¹⁴. However, there is a controversy about the phase diagram with respect to the normal-state pseudogap line². On the one hand, some authors¹⁵ analyzed the experimental data, and then they argued that the normal-state pseudogap line intersects the SC dome at about optimal doping. On the other hand, it has been argued that the normal-state pseudogap merges gradually with the SC gap in the overdoped regime¹⁶, eventually disappearing together with superconductivity at the doping levels larger than $\delta \sim 0.27$. Theoretically, to the best of our knowledge, all theoretical studies of the normal-state pseudogap phenomenon and its relevance to superconductivity performed so far are based on the phenomenological d-wave Bardeen-Cooper-Schrieffer (BCS) formalism¹⁵⁻¹⁸. In particular, a phenomenological theory of the normal-

state pseudogap state has been developed¹⁹, where an ansatz is proposed for the coherent part of the single particle Green's function in a doped resonant valence bond state, and then the calculated result of the electronic properties in the normal-state pseudogap phase is in qualitative agreement with the experimental data. Moreover, it has been argued recently that the pseudogap is a combination of a quantum disordered d-wave superconductor and an entirely different form of competing order, originating from the particle-hole channel²⁰. However, up to now, the interplay between the SC gap and normal-state pseudogap in cuprate superconductors has not been treated starting from a microscopic SC theory, therefore no general consensus for the normal-state pseudogap has been reached yet on its origin, its role in the onset of superconductivity itself, and not even on its evolution across the phase diagram of cuprate superconductors².

In our earlier work, a kinetic energy driven SC mechanism has been developed²¹, where the interaction between charge carriers and spins directly from the kinetic energy by exchanging spin excitations in the higher power of the doping concentration induces a d-wave charge carrier pairing state, and then their condensation reveals the SC ground-state. In particular, this SC-state is controlled by both the SC gap and quasiparticle coherence, which leads to that the maximal SC transition temperature occurs around the optimal doping, and then decreases in both the underdoped and overdoped regimes. Within this kinetic energy driven SC mechanism, we have discussed the low energy electronic structure²², quasiparticle transport²³, and Meissner effect²⁴, and qualitatively reproduced some main features of the corresponding experimental results of cuprate superconductors in the SC-state. In this paper, we study the interplay between the SC gap and normal-state pseudogap in cuprate superconductors based on this kinetic energy driven SC mechanism²¹, where one of our main results is that the interaction between charge carriers and spins directly from the kinetic energy by exchanging spin excitations in the higher power of the doping concentration induces the normal-state pseudogap state in the particle-hole channel

and SC-state in the particle-particle channel, therefore there is a coexistence of the SC gap and normal-state pseudogap in the whole SC dome. Our results also show that both the pseudogap and SC gap are dominated by one energy scale, and the normal-state pseudogap also is a necessary ingredient for superconductivity in cuprate superconductors.

We start from the t - J model on a square lattice²⁵,

$$H = -t \sum_{i\hat{\eta}\sigma} C_{i\sigma}^\dagger C_{i+\hat{\eta}\sigma} + t' \sum_{i\hat{\tau}\sigma} C_{i\sigma}^\dagger C_{i+\hat{\tau}\sigma} + \mu \sum_{i\sigma} C_{i\sigma}^\dagger C_{i\sigma} + J \sum_{i\hat{\eta}} \mathbf{S}_i \cdot \mathbf{S}_{i+\hat{\eta}}, \quad (1)$$

where $\hat{\eta} = \pm\hat{x}, \pm\hat{y}$, $\hat{\tau} = \pm\hat{x} \pm \hat{y}$, $C_{i\sigma}^\dagger$ ($C_{i\sigma}$) is the electron creation (annihilation) operator, $\mathbf{S}_i = (S_i^x, S_i^y, S_i^z)$ are spin operators, and μ is the chemical potential. This t - J model (1) is subject to an important local constraint $\sum_\sigma C_{i\sigma}^\dagger C_{i\sigma} \leq 1$ to avoid the double occupancy. To incorporate this electron single occupancy local constraint, the charge-spin separation (CSS) fermion-spin theory²⁶ has been proposed, where the physics of no double occupancy is taken into account by representing the electron as a composite object created by $C_{i\uparrow} = h_{i\uparrow}^\dagger S_i^-$ and $C_{i\downarrow} = h_{i\downarrow}^\dagger S_i^+$, with the spinful fermion operator $h_{i\sigma} = e^{-i\Phi_{i\sigma}} h_i$ that describes the charge degree of freedom of the electron together with some effects of spin configuration rearrangements due to the presence of the doped hole itself (charge carrier), while the spin operator S_i represents the spin degree of freedom of the electron, then the electron single occupancy local constraint is satisfied in analytical calculations. In this CSS fermion-spin representation, the t - J model (1) can be expressed as^{21,26},

$$H = t \sum_{i\hat{\eta}} (h_{i+\hat{\eta}\uparrow}^\dagger h_{i\uparrow} S_i^+ S_{i+\hat{\eta}}^- + h_{i+\hat{\eta}\downarrow}^\dagger h_{i\downarrow} S_i^- S_{i+\hat{\eta}}^+) - t' \sum_{i\hat{\tau}} (h_{i+\hat{\tau}\uparrow}^\dagger h_{i\uparrow} S_i^+ S_{i+\hat{\tau}}^- + h_{i+\hat{\tau}\downarrow}^\dagger h_{i\downarrow} S_i^- S_{i+\hat{\tau}}^+) - \mu \sum_{i\sigma} h_{i\sigma}^\dagger h_{i\sigma} + J_{\text{eff}} \sum_{i\hat{\eta}} \mathbf{S}_i \cdot \mathbf{S}_{i+\hat{\eta}}, \quad (2)$$

where $J_{\text{eff}} = (1 - \delta)^2 J$, and $\delta = \langle h_{i\sigma}^\dagger h_{i\sigma} \rangle = \langle h_i^\dagger h_i \rangle$ is the doping concentration. As a consequence, the kinetic energy in the t - J model has been transferred as the interaction between charge carriers and spins, which reflects that even the kinetic energy in the t - J model has strong Coulombic contribution due to the restriction of single occupancy of a given site. In this case, we²¹ have shown in terms of Eliashberg's strong coupling theory²⁷ that in the case without AFLRO, this interaction between charge carriers and spins by exchanging spin excitations in the higher power of the doping concentration can induce the d-wave charge carrier pairing state (then the d-wave electron Cooper pairing state). Following our previous discussions²¹, the self-consistent equations that satisfied by the full charge carrier diagonal and

off-diagonal Green's functions are obtained as,

$$g(k) = g^{(0)}(k) + g^{(0)}(k)[\Sigma_1^{(h)}(k)g(k) - \Sigma_2^{(h)}(-k)\Gamma^\dagger(k)], \quad (3a)$$

$$\Gamma^\dagger(k) = g^{(0)}(-k)[\Sigma_1^{(h)}(-k)\Gamma^\dagger(-k) + \Sigma_2^{(h)}(-k)g(k)], \quad (3b)$$

respectively, where the four-vector notation $k = (\mathbf{k}, i\omega_n)$, and the charge carrier mean-field (MF) Green's function^{21,22}, $g^{(0)-1}(k) = i\omega_n - \xi_{\mathbf{k}}$, with the MF charge carrier spectrum $\xi_{\mathbf{k}} = Zt\chi_1\gamma_{\mathbf{k}} - Zt'\chi_2\gamma'_{\mathbf{k}} - \mu$, the spin correlation functions $\chi_1 = \langle S_i^+ S_{i+\hat{\eta}}^- \rangle$, $\chi_2 = \langle S_i^+ S_{i+\hat{\tau}}^- \rangle$, $\gamma_{\mathbf{k}} = (1/Z) \sum_{\hat{\eta}} e^{i\mathbf{k}\cdot\hat{\eta}}$, $\gamma'_{\mathbf{k}} = (1/Z) \sum_{\hat{\tau}} e^{i\mathbf{k}\cdot\hat{\tau}}$, and Z is the number of the nearest neighbor or next-nearest neighbor sites, while the self-energies $\Sigma_1^{(h)}(k)$ in the particle-hole channel and $\Sigma_2^{(h)}(k)$ in the particle-particle channel have been evaluated from the spin bubble as,

$$\Sigma_1^{(h)}(k) = \frac{1}{N^2} \sum_{\mathbf{p}, \mathbf{p}'} \Lambda_{\mathbf{p}+\mathbf{p}'+\mathbf{k}}^2 \times \frac{1}{\beta} \sum_{ip_m} g(p+k)\Pi(\mathbf{p}, \mathbf{p}', ip_m), \quad (4a)$$

$$\Sigma_2^{(h)}(k) = \frac{1}{N^2} \sum_{\mathbf{p}, \mathbf{p}'} \Lambda_{\mathbf{p}+\mathbf{p}'+\mathbf{k}}^2 \times \frac{1}{\beta} \sum_{ip_m} \Gamma^\dagger(-p-k)\Pi(\mathbf{p}, \mathbf{p}', ip_m), \quad (4b)$$

where $\Lambda_{\mathbf{k}} = Zt\gamma_{\mathbf{k}} - Zt'\gamma'_{\mathbf{k}}$, and the spin bubble,

$$\Pi(\mathbf{p}, \mathbf{p}', ip_m) = \frac{1}{\beta} \sum_{ip'_m} D^{(0)}(p')D^{(0)}(p' + p), \quad (5)$$

where $p = (\mathbf{p}, ip_m)$, $p' = (\mathbf{p}', ip'_m)$, and the MF spin Green's function, $D^{(0)-1}(p) = [(ip_m)^2 - \omega_{\mathbf{p}}^2]/B_{\mathbf{p}}$, with the MF spin excitation spectrum $\omega_{\mathbf{p}}$ and $B_{\mathbf{p}}$ have been given in Ref. 22.

Since the pairing force and charge carrier pair gap have been incorporated into the charge carrier self-energy $\Sigma_2^{(h)}(k)$ in the particle-particle channel, then it is called as the effective charge carrier pair gap $\bar{\Delta}_h(k) = \Sigma_2^{(h)}(k)$. On the other hand, the charge carrier self-energy $\Sigma_1^{(h)}(k)$ in the particle-hole channel renormalizes the MF charge carrier spectrum²⁸. In particular, $\Sigma_2^{(h)}(k)$ is an even function of $i\omega_n$, while $\Sigma_1^{(h)}(k)$ is not. In our previous discussions²¹, $\Sigma_1^{(h)}(k)$ has been broken up into its symmetric and antisymmetric parts as, $\Sigma_1^{(h)}(k) = \Sigma_{1e}^{(h)}(k) + i\omega_n \Sigma_{1o}^{(h)}(k)$, then both $\Sigma_{1e}^{(h)}(k)$ and $\Sigma_{1o}^{(h)}(k)$ are an even function of $i\omega_n$. In this case, we have defined the charge carrier quasiparticle coherent weight $Z_{hF}^{-1}(k) = 1 - \text{Re}\Sigma_{1o}^{(h)}(k)$, then in the static limit approximation for the effective charge carrier pair gap and quasiparticle coherent weight, i.e., $\bar{\Delta}_h(k) = \bar{\Delta}_h \gamma_{\mathbf{k}}^{(d)}$ with $\gamma_{\mathbf{k}}^{(d)} = (\cos k_x - \cos k_y)/2$, and

$Z_{\text{hF}}^{-1} = 1 - \text{Re}\Sigma_{10}^{(\text{h})}(\mathbf{k}, \omega = 0)|_{\mathbf{k}=[\pi, 0]}$, the BCS-like charge carrier diagonal and off-diagonal Green's functions with the d-wave symmetry have been obtained^{21,22}, although the pairing mechanism is driven by the kinetic energy by exchanging spin excitations. With the help of these

charge carrier diagonal and off-diagonal Green's functions, $\Sigma_1^{(\text{h})}(k)$ and $\bar{\Delta}_h(\mathbf{k})$ in Eq. (4) have been obtained explicitly as^{21,22},

$$\Sigma_1^{(h)}(k) = \frac{1}{N^2} \sum_{\mathbf{p}\mathbf{p}'\mu\nu\tau} \Lambda_{\mathbf{p}+\mathbf{p}'+\mathbf{k}}^2 \frac{B_{\mathbf{p}'}B_{\mathbf{p}'+\mathbf{k}}}{8\omega_{\mu\mathbf{p}'}\omega_{\nu\mathbf{p}'+\mathbf{k}}} \left(1 + \frac{\bar{\xi}_{\mathbf{p}+\mathbf{k}}}{E_{\mathbf{h}\mathbf{p}+\mathbf{k}}^{(\tau)}}\right) \frac{F_{\mu\nu\tau}(\mathbf{p}, \mathbf{p}', \mathbf{k})}{i\omega_n + \omega_{\nu\mathbf{p}'+\mathbf{k}} - \omega_{\mu\mathbf{p}'} - E_{\mathbf{h}\mathbf{p}+\mathbf{k}}^{(\tau)}}, \quad (6a)$$

$$\bar{\Delta}_h(\mathbf{k}) = \frac{1}{N^2} \sum_{\mathbf{p}\mathbf{p}'\mu\nu\tau} \Lambda_{\mathbf{p}+\mathbf{p}'+\mathbf{k}}^2 \frac{B_{\mathbf{p}'}B_{\mathbf{p}'+\mathbf{k}}}{8\omega_{\mu\mathbf{p}'}\omega_{\nu\mathbf{p}'+\mathbf{k}}} \frac{\bar{\Delta}_{\text{hZ}}(\mathbf{p}+\mathbf{k})}{E_{\mathbf{h}\mathbf{p}+\mathbf{k}}^{(\tau)}} \frac{F_{\mu\nu\tau}(\mathbf{p}, \mathbf{p}', \mathbf{k})}{\omega_{\nu\mathbf{p}'+\mathbf{k}} - \omega_{\mu\mathbf{p}'} - E_{\mathbf{h}\mathbf{p}+\mathbf{k}}^{(\tau)}}, \quad (6b)$$

where $F_{\mu\nu\tau}(\mathbf{p}, \mathbf{p}', \mathbf{k}) = Z_{\text{hF}}\{n_F(E_{\mathbf{h}\mathbf{p}+\mathbf{k}}^{(\tau)})[n_B(\omega_{\mu\mathbf{p}'}) - n_B(\omega_{\nu\mathbf{p}'+\mathbf{k}})] + n_B(\omega_{\nu\mathbf{p}'+\mathbf{k}})[1 + n_B(\omega_{\mu\mathbf{p}'})]\}$, $\mu, \nu, \tau = 1, 2$, $\omega_{1\mathbf{p}} = \omega_{\mathbf{p}}$, $\omega_{2\mathbf{p}} = -\omega_{\mathbf{p}}$, $E_{\text{h}\mathbf{k}}^{(1)} = E_{\text{h}\mathbf{k}}$, $E_{\text{h}\mathbf{k}}^{(2)} = -E_{\text{h}\mathbf{k}}$, the renormalized charge carrier excitation spectrum $\bar{\xi}_{\mathbf{k}} = Z_{\text{hF}}\xi_{\mathbf{k}}$, the renormalized charge carrier pair gap $\bar{\Delta}_{\text{hZ}}(\mathbf{k}) = Z_{\text{hF}}\bar{\Delta}_h(\mathbf{k})$, the charge carrier quasiparticle spectrum $E_{\text{h}\mathbf{k}} = \sqrt{\bar{\xi}_{\mathbf{k}}^2 + |\bar{\Delta}_{\text{hZ}}(\mathbf{k})|^2}$, and $n_B(\omega_{\mathbf{p}})$ and $n_F(E_{\text{h}\mathbf{k}})$ are the boson and fermion distribution functions, respectively.

However, in fact, the charge carrier self-energy $\Sigma_1^{(\text{h})}(k)$ in the particle-hole channel in Eq. (6) also can be rewritten as,

$$\Sigma_1^{(h)}(k) = \frac{[2\bar{\Delta}_R(\mathbf{k})]^2}{i\omega_n + M_{\mathbf{k}}}, \quad (7)$$

where as in the case of the effective charge carrier pair gap, the interaction force and normal-state pseudogap have been incorporated into $\bar{\Delta}_R(\mathbf{k})$, then it is called as

the effective normal-state pseudogap, while $M_{\mathbf{k}}$ is the energy spectrum of $\Sigma_1^{(\text{h})}(k)$. In this case, it is obvious that in our previous static limit approximation^{21,22} for $\Sigma_{10}^{(\text{h})}(k)$, the quasiparticle coherent weight $Z_{\text{hF}}^{-1} = \{1 + [2\bar{\Delta}_R(\mathbf{k})]^2/M_{\mathbf{k}}^2\}|_{\mathbf{k}=[\pi, 0]}$, which reflects that the partial effect of the normal-state pseudogap has been contained in the quasiparticle coherent weight. Since the SC-state in the kinetic energy driven SC mechanism is controlled by both the SC gap and quasiparticle coherence²¹, then in this sense, the normal-state pseudogap is a necessary ingredient for superconductivity in cuprate superconductors. In the following discussions, we focus on the connection between the normal-state pseudogap and SC gap beyond our previous static limit approximation²¹ for the charge carrier self-energy $\Sigma_1^{(\text{h})}(k)$ in the particle-hole channel, and show explicitly the two-gap feature in cuprate superconductors. In this case, the full charge carrier diagonal and off-diagonal Green's functions can be evaluated from Eqs. (3) and (7) as,

$$g(k) = \frac{1}{i\omega_n - \xi_{\mathbf{k}} - \Sigma_1^{(\text{h})}(k) - \bar{\Delta}_h^2(\mathbf{k})/[i\omega_n + \xi_{\mathbf{k}} + \Sigma_1^{(\text{h})}(-k)]} = \frac{U_{1\text{h}\mathbf{k}}^2}{i\omega_n - E_{1\text{h}\mathbf{k}}} + \frac{V_{1\text{h}\mathbf{k}}^2}{i\omega_n + E_{1\text{h}\mathbf{k}}} + \frac{U_{2\text{h}\mathbf{k}}^2}{i\omega_n - E_{2\text{h}\mathbf{k}}} + \frac{V_{2\text{h}\mathbf{k}}^2}{i\omega_n + E_{2\text{h}\mathbf{k}}}, \quad (8a)$$

$$\Gamma^{\dagger}(k) = -\frac{\bar{\Delta}_h(\mathbf{k})}{[i\omega_n - \xi_{\mathbf{k}} - \Sigma_1^{(\text{h})}(k)][i\omega_n + \xi_{\mathbf{k}} + \Sigma_1^{(\text{h})}(-k)] - \bar{\Delta}_h^2(\mathbf{k})} = -\frac{1}{E_{1\text{h}\mathbf{k}}^2 - E_{2\text{h}\mathbf{k}}^2} \left[\frac{\bar{\Delta}_h(\mathbf{k})}{2E_{1\text{h}\mathbf{k}}} \left(\frac{1}{i\omega_n - E_{1\text{h}\mathbf{k}}} - \frac{1}{i\omega_n + E_{1\text{h}\mathbf{k}}} \right) - \frac{\bar{\Delta}_h(\mathbf{k})}{2E_{2\text{h}\mathbf{k}}} \left(\frac{1}{i\omega_n - E_{2\text{h}\mathbf{k}}} - \frac{1}{i\omega_n + E_{2\text{h}\mathbf{k}}} \right) \right], \quad (8b)$$

where there are four branches of the charge carrier quasiparticle spectrum due to the presence of the normal-state pseudogap and SC gap, $E_{1\text{h}\mathbf{k}}$, $-E_{1\text{h}\mathbf{k}}$, $E_{2\text{h}\mathbf{k}}$, and $-E_{2\text{h}\mathbf{k}}$, with $E_{1\text{h}\mathbf{k}} = \sqrt{[\Omega_{\mathbf{k}} + \Theta_{\mathbf{k}}]/2}$, $E_{2\text{h}\mathbf{k}} = \sqrt{[\Omega_{\mathbf{k}} - \Theta_{\mathbf{k}}]/2}$, and the

kernel functions,

$$\Omega_{\mathbf{k}} = \xi_{\mathbf{k}}^2 + M_{\mathbf{k}}^2 + 8\bar{\Delta}_R^2(\mathbf{k}) + \bar{\Delta}_h^2(\mathbf{k}), \quad (9a)$$

$$\Theta_{\mathbf{k}} = \sqrt{(\xi_{\mathbf{k}}^2 - M_{\mathbf{k}}^2)[\xi_{\mathbf{k}}^2 - M_{\mathbf{k}}^2 + 2\bar{\Delta}_h^2(\mathbf{k})] + 16\bar{\Delta}_R^2(\mathbf{k})[(\xi_{\mathbf{k}} - M_{\mathbf{k}})^2 + \bar{\Delta}_h^2(\mathbf{k})] + \bar{\Delta}_h^4(\mathbf{k})}, \quad (9b)$$

while the coherence factors,

$$U_{1h\mathbf{k}}^2 = \frac{1}{2(E_{1h\mathbf{k}}^2 - E_{2h\mathbf{k}}^2)} \left[(E_{1h\mathbf{k}}^2 - M_{\mathbf{k}}^2) \left(1 + \frac{\xi_{\mathbf{k}}}{E_{1h\mathbf{k}}} \right) - [2\bar{\Delta}_R(\mathbf{k})]^2 \left(1 + \frac{M_{\mathbf{k}}}{E_{1h\mathbf{k}}} \right) \right], \quad (10a)$$

$$V_{1h\mathbf{k}}^2 = \frac{1}{2(E_{1h\mathbf{k}}^2 - E_{2h\mathbf{k}}^2)} \left[(E_{1h\mathbf{k}}^2 - M_{\mathbf{k}}^2) \left(1 - \frac{\xi_{\mathbf{k}}}{E_{1h\mathbf{k}}} \right) - [2\bar{\Delta}_R(\mathbf{k})]^2 \left(1 - \frac{M_{\mathbf{k}}}{E_{1h\mathbf{k}}} \right) \right], \quad (10b)$$

$$U_{2h\mathbf{k}}^2 = -\frac{1}{2(E_{1h\mathbf{k}}^2 - E_{2h\mathbf{k}}^2)} \left[(E_{2h\mathbf{k}}^2 - M_{\mathbf{k}}^2) \left(1 + \frac{\xi_{\mathbf{k}}}{E_{2h\mathbf{k}}} \right) - [2\bar{\Delta}_R(\mathbf{k})]^2 \left(1 + \frac{M_{\mathbf{k}}}{E_{2h\mathbf{k}}} \right) \right], \quad (10c)$$

$$V_{2h\mathbf{k}}^2 = -\frac{1}{2(E_{1h\mathbf{k}}^2 - E_{2h\mathbf{k}}^2)} \left[(E_{2h\mathbf{k}}^2 - M_{\mathbf{k}}^2) \left(1 - \frac{\xi_{\mathbf{k}}}{E_{2h\mathbf{k}}} \right) - [2\bar{\Delta}_R(\mathbf{k})]^2 \left(1 - \frac{M_{\mathbf{k}}}{E_{2h\mathbf{k}}} \right) \right], \quad (10d)$$

satisfy the sum rule: $U_{1h\mathbf{k}}^2 + V_{1h\mathbf{k}}^2 + U_{2h\mathbf{k}}^2 + V_{2h\mathbf{k}}^2 = 1$, and the corresponding effective normal-state pseudogap $\bar{\Delta}_R(\mathbf{k})$ and energy spectrum $M_{\mathbf{k}}$ in Eq. (7) can be obtained explicitly in terms of the self-energy $\Sigma_1^{(h)}(k)$ in Eq. (6) as,

$$\bar{\Delta}_R(\mathbf{k}) = \frac{L_2(\mathbf{k})}{2\sqrt{L_1(\mathbf{k})}}, \quad (11a)$$

$$M_{\mathbf{k}} = \frac{L_2(\mathbf{k})}{L_1(\mathbf{k})}, \quad (11b)$$

with $L_1(\mathbf{k})$ and $L_2(\mathbf{k})$ are given by,

$$L_1(\mathbf{k}) = \frac{1}{N^2} \sum_{\mathbf{p}\mathbf{p}'\mu\nu\tau} \Lambda_{\mathbf{p}+\mathbf{p}'+\mathbf{k}}^2 \frac{B_{\mathbf{p}'}B_{\mathbf{p}'+\mathbf{p}}}{8\omega_{\mu\mathbf{p}'}\omega_{\nu\mathbf{p}'+\mathbf{p}}} \left(1 + \frac{\bar{\xi}_{\mathbf{p}+\mathbf{k}}}{E_{\mathbf{h}\mathbf{p}+\mathbf{k}}^{(\tau)}} \right) \frac{F_{\mu\nu\tau}(\mathbf{p}, \mathbf{p}', \mathbf{k})}{[\omega_{\nu\mathbf{p}'+\mathbf{p}} - \omega_{\mu\mathbf{p}'} - E_{\mathbf{h}\mathbf{p}+\mathbf{k}}^{(\tau)}]^2}, \quad (12a)$$

$$L_2(\mathbf{k}) = \frac{1}{N^2} \sum_{\mathbf{p}\mathbf{p}'\mu\nu\tau} \Lambda_{\mathbf{p}+\mathbf{p}'+\mathbf{k}}^2 \frac{B_{\mathbf{p}'}B_{\mathbf{p}'+\mathbf{p}}}{8\omega_{\mu\mathbf{p}'}\omega_{\nu\mathbf{p}'+\mathbf{p}}} \left(1 + \frac{\bar{\xi}_{\mathbf{p}+\mathbf{k}}}{E_{\mathbf{h}\mathbf{p}+\mathbf{k}}^{(\tau)}} \right) \frac{F_{\mu\nu\tau}(\mathbf{p}, \mathbf{p}', \mathbf{k})}{\omega_{\nu\mathbf{p}'+\mathbf{p}} - \omega_{\mu\mathbf{p}'} - E_{\mathbf{h}\mathbf{p}+\mathbf{k}}^{(\tau)}}, \quad (12b)$$

then it is straightforward to obtain the magnitude of the effective normal-state pseudogap from Eq. (11) as $\bar{\Delta}_R = (1/N) \sum_{\mathbf{k}} \bar{\Delta}_R(\mathbf{k})$.

Now we are ready to discuss the interplay between the SC gap and normal-state pseudogap in cuprate superconductors. In cuprate superconductors, although the values of J , t , and t' are believed to vary somewhat from compound to compound⁴, however, as a qualitative discussion, the commonly used parameters in this paper are chosen as $t/J = 2.5$, $t'/t = 0.3$, and $J = 110$ meV. In this case, the magnitude of the effective normal-state pseudogap ($2\bar{\Delta}_R$) (solid line) and effective charge carrier pair gap parameter ($2\bar{\Delta}_h$) (dashed line) as a function of doping for temperature $T = 0.002J$ are plotted in Fig. 1 in comparison with the corresponding experimental data² of cuprate superconductors (inset). Obviously, the two-gap feature observed from cuprate superconductors² is qualitatively reproduced. In particular, the result of the effective charge carrier pair gap parameter (then the SC gap parameter) is the same with our previous work^{21,22}, i.e., it increases with increasing the doping concentration in the underdoped regime, and reaches a maximum

in the optimal doping, then decreases in the overdoped regime. However, in contrast to the case of the effective charge carrier pair gap parameter in the underdoped regime, the magnitude of the effective normal-state pseudogap smoothly increases with decreasing the doping concentration in the underdoped regime, this leads to that the magnitude of the effective normal-state pseudogap is much larger than the effective charge carrier pair gap parameter in the underdoped regime. Moreover, the magnitude of the normal-state pseudogap seems to merge with the charge carrier pair gap parameter in the overdoped regime, eventually disappearing together with superconductivity at the doping concentrations larger than $\delta \sim 0.27$, in qualitative agreement with the experimental results².

As in the temperature dependence of the SC gap, this normal-state pseudogap is also temperature dependent. In particular, in the given doping concentration, the normal-state pseudogap vanishes when temperature

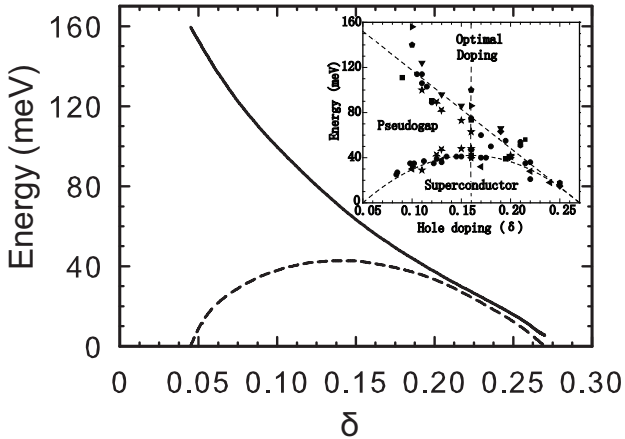


FIG. 1: The magnitude of the effective normal-state pseudogap ($2\bar{\Delta}_R$) (solid line) and effective charge carrier pair gap parameter ($2\bar{\Delta}_h$) (dashed line) as a function of doping for temperature $T = 0.002J$ with parameters $t/J = 2.5$, $t'/t = 0.3$, and $J = 110\text{meV}$. Inset: the corresponding experimental data of cuprate superconductors taken from Ref. 2.

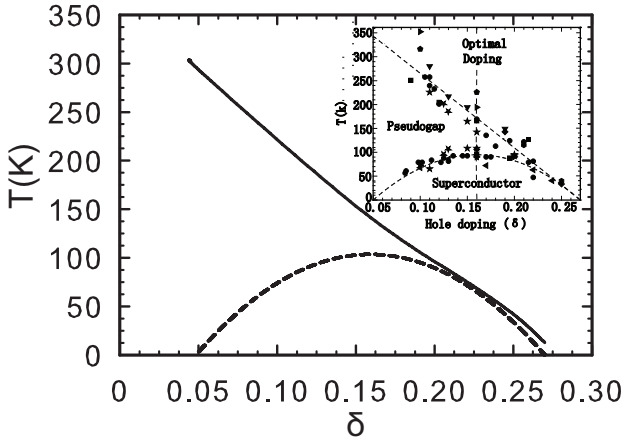


FIG. 2: The normal-state pseudogap crossover temperature T^* (solid line) and superconducting transition temperature T_c (dashed line) as a function of doping for parameters $t/J = 2.5$, $t'/t = 0.3$, and $J = 110\text{meV}$. Inset: the corresponding experimental data of cuprate superconductors taken from Ref. 2.

reaches the normal-state pseudogap crossover temperature T^* . To show this doping dependence of the normal-state pseudogap crossover temperature T^* clearly, we have made a series of calculations for T^* at different doping concentrations, and the results of the normal-state pseudogap crossover temperature T^* (solid line) and SC transition temperature T_c (dashed line) as a function of doping are plotted in Fig. 2 in comparison with the corresponding experimental data of cuprate superconductors². Our result shows clearly that in corresponding to the result of the doping dependence of the normal-state pseudogap shown in Fig. 1, the normal-state pseudogap crossover temperature T^* is much larger

than the SC transition temperature T_c in the under-doped regime, then it smoothly decreases with increasing the doping. Moreover, both the normal-state pseudogap crossover temperature T^* and SC transition temperature T_c converge to the almost same doping concentration $\delta \sim 0.27$ at the end of the SC dome, also in qualitative agreement with the experimental results².

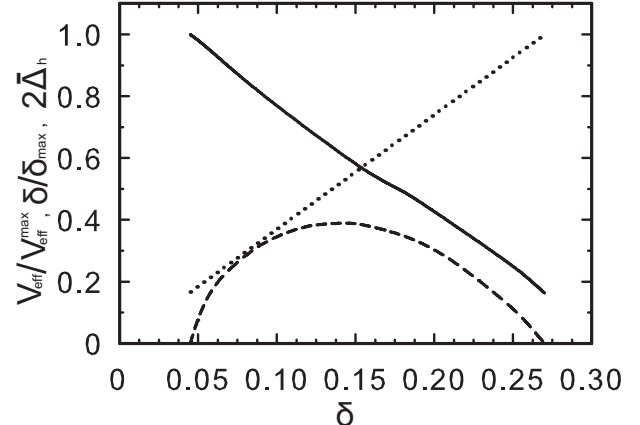


FIG. 3: The strength of the attractive interaction (solid line), the doping (dotted line), and the effective charge carrier pair gap parameter ($2\bar{\Delta}_h$) (dashed line) as a function of doping for temperature $T = 0.002J$ with parameters $t/J = 2.5$, $t'/t = 0.3$, and $J = 110\text{meV}$.

Our present results in Fig. 1 and Fig. 2 show clearly that there are two coexisting energy gaps in the whole SC dome: one associated with a direct measure of the binding energy of the two electrons forming a Cooper pair²¹, while the other with the anomalous normal-state properties^{14,19}. Within the kinetic energy driven SC mechanism²¹, the essential physics of this two-gap feature in cuprate superconductors can be attributed to the doping dependence of the charge carrier interactions in the particle-hole and particle-particle channels induced by exchanging spin excitations in the higher power of the doping concentration. The parent compounds of cuprate superconductors are the Mott insulators⁴ as we have mentioned above, when charge carriers are doped into a Mott insulator, there is a gain in the kinetic energy per charge carrier proportional to t due to hopping, but at the same time, the magnetic energy is decreased, costing an energy of approximately J per site, therefore the doped charge carriers into a Mott insulator can be considered as a competition between the kinetic energy (δt) and magnetic energy (J), and then the spectral strength of the spin excitation decreases with increasing the doping. In the particle-particle channel, the charge carriers (then the electrons) interact by exchanging spin excitations in the higher power of the doping concentration, and then this interaction is attractive. This attractive interaction leads to form the charge carrier pairs (then the electron Cooper pairs)²¹. Since the pairing force and charge carrier pair gap have been incorporated into the

effective charge carrier pair gap²¹ as mentioned above, the strength V_{eff} of this attractive interaction can be obtained in terms of the effective charge carrier pair gap parameter $\bar{\Delta}_h$ and charge carrier pair gap parameter Δ_h as $V_{\text{eff}} = \bar{\Delta}_h / \Delta_h$, where Δ_h is evaluated in terms of the charge carrier off-diagonal Green's function, and has been given in Refs. 21 and 22. In this case, the decrease of the spectral strength of the spin excitation with increasing the doping concentration leads to a decrease of the coupling strength V_{eff} . To see this point clearly, we have calculated the doping dependence of V_{eff} , and the results of $V_{\text{eff}}/V_{\text{eff}}^{\text{max}}$ (solid line), $\delta/\delta_{\text{max}}$ (dotted line), and $2\bar{\Delta}_h$ (dashed line) as a function of doping for $T = 0.002J$ are plotted in Fig. 3, where $V_{\text{eff}}^{\text{max}} = V_{\text{eff}}|_{\delta=0.045}$ is the value of V_{eff} at the starting point of the SC dome, while $\delta_{\text{max}} = 0.27$ is the doping concentration at the end point of the SC dome. It is therefore shown that the coupling strength V_{eff} smoothly decreases upon increasing the doping from the strong-coupling case in the underdoped regime to a weak-coupling side in the overdoped regime. Moreover, in the underdoped regime, the strength V_{eff} of the attractive interaction mediated by spin excitations is rather strong to form the charge carrier pairs (then the electron Cooper pairs) for the most charge carriers (then the electrons), therefore the number of the charge carrier pairs (then the electron Cooper pairs) and the charge carrier pair gap parameter (then the SC transition temperature) are increase with increasing the doping concentration. However, in the overdoped regime, the coupling strength V_{eff} is relatively weak, and in this case, not all charge carriers (then the electrons) can be bounden as the charge carrier pairs (then the electron Cooper pairs) by the weak attractive interaction, and therefore the number of the charge carrier pairs (then the electron Cooper pairs) and the charge carrier pair gap parameter (then the SC transition temperature) decrease with increasing the doping concentration. In particular, the optimal doping is a balance point, where the doping concentration (then the kinetic energy) and the coupling strength V_{eff} are optimally matched. These physical properties lead to that the maximal charge carrier pair gap parameter (then the SC transition temperature) occurs around the optimal doping, and then decreases in both the underdoped and overdoped regimes²¹. On the other hand, in the particle-hole channel, the charge carriers (then the electrons) also interact by exchanging spin excitations in the higher power of the doping concentration as in the case of the particle-particle channel. This interaction in the particle-hole channel reduces the charge carrier quasiparticle (then the electron quasiparticle) bandwidth²⁸, and therefore the energy scale of the electron quasiparticle band is controlled by the magnetic interaction J . In this case, the magnitude of the effective normal-state pseudogap $\bar{\Delta}_R$ (then the normal-state pseudogap crossover temperature T^*) originated from the self-energy $\Sigma_1^{(h)}(k)$ in the particle-hole channel has the same doping dependent behavior of V_{eff} , i.e., it reaches its maximum at the start-

ing point of the SC dome, and then decreases with increasing the doping concentration, eventually disappearing at the end point of the SC dome. Furthermore, since the charge carrier interactions in both the particle-hole and particle-particle channels are mediated by spin excitations in the higher power of the doping concentration, and therefore all these charge carrier interactions in both the particle-hole and particle-particle channels are controlled by the magnetic interaction J . In this sense, both the normal-state pseudogap (then the normal-state pseudogap crossover temperature) and SC gap (then the SC transition temperature) in the phase diagram of cuprate superconductors shown in Fig. 1 (then Fig. 2) are dominated by one energy scale. Moreover, our present theory starting from the t - J model also shows that both the normal-state pseudogap and SC gap are the result of the strong electron correlation in cuprate superconductors.

In conclusion, we have discussed the interplay between the SC gap and normal-state pseudogap in cuprate superconductors based on the kinetic energy driven SC mechanism. Our results show that the interaction between charge carriers and spins directly from the kinetic energy by exchanging spin excitations in the higher power of the doping concentration induces the normal-state pseudogap state in the particle-hole channel and SC-state in the particle-particle channel, therefore there is a coexistence of the SC gap and normal-state pseudogap in the whole SC dome. This normal-state pseudogap is closely related to the quasiparticle coherent weight, and is a necessary ingredient for superconductivity in cuprate superconductors. Our results also show that both the normal-state pseudogap and SC gap are dominated by one energy scale, and they are the result of the strong electron correlation.

Recently, the specific-heat measurement²⁹ on the cuprate superconductor $\text{Bi}_2\text{Sr}_{2-x}\text{La}_x\text{CuO}_{6+\delta}$ shows that the specific-heat coefficient has a humplike anomaly at the SC transition temperature T_c , and behaves as a long tail which persists far into the normal-state in the underdoped regime, but in the heavily overdoped regime the anomaly ends sharply just near T_c . In this case, we³⁰ have studied the doping dependence of the thermodynamic properties in cuprate superconductors within the present framework, and the results show that this humplike anomaly in the underdoped regime is closely related to the normal-state pseudogap. These and the related results will be presented elsewhere.

Acknowledgments

The authors would like to thank Dr. Yu Lan for the help in the numerical calculations. This work was supported by the National Natural Science Foundation of China under Grant No. 11074023, and the funds from the Ministry of Science and Technology of China under Grant Nos. 2011CB921700 and 2012CB821403.

^{*} To whom correspondence should be addressed, E-mail: spfeng@bnu.edu.cn

² See, e.g., S. Hüfner, M. A. Hossain, A. Damascelli, and G. A. Sawatzky, *Rep. Prog. Phys.* **71**, 062501 (2008), and references therein.

³ See, e.g., Tom Timusk and Bryan Statt, *Rep. Prog. Phys.* **62**, 61 (1999), and references therein.

⁴ See, e.g., A. Damascelli, Z. Hussain, and Z.-X. Shen, *Rev. Mod. Phys.* **75**, 473 (2003), and references therein.

⁵ See, e.g., Guy Deutscher, *Rev. Mod. Phys.* **77**, 109 (2005), and references therein.

⁶ See, e.g., Matthias Eschrig, *Adv. Phys.* **55**, 47 (2006).

⁷ See, e.g., T. P. Devereaux and R. Hackl, *Rev. Mod. Phys.* **79**, 175 (2007).

⁸ See, e.g., Øystein Fischer, Martin Kugler, Ivan Maggio-Aprile, Christophe Berthod, and Christoph Renner, *Rev. Mod. Phys.* **79**, 353 (2007), and references therein.

⁹ B. Batlogg, H.Y. Hwang, H. Takagi, R.J. Cava, H.L. Kao, and J. Kwo, *Physica C* **235-240**, 130 (1994).

¹⁰ A. G. Loeser, Z.-X. Shen, D. S. Dessau, D. S. Marshall, C. H. Park, P. Fournier, and A. Kapitulnik, *Science* **273**, 325 (1996); H. Ding, T. Yokoya, J. C. Campuzano, T. Takahashi, M. Randeria, M. R. Norman, T. Mochiku, K. Kadouwaki and J. Giapintzakis, *Nature* **382**, 51 (1996); Takeshi Kondo, Tsunehiro Takeuchi, Adam Kaminski, Syunsuke Tsuda, and Shik Shin, *Phys. Rev. Lett.* **98**, 267004 (2007); W. S. Lee, I. M. Vishik, K. Tanaka, D. H. Lu, T. Sasagawa, N. Nagaosa, T. P. Devereaux, Z. Hussain and Z.-X. Shen, *Nature* **450**, 81 (2007); M. Hashimoto, R.-H. He, K. Tanaka, J. P. Testaud, W. Meevasana, R. G. Moore, D. H. Lu, H. Yao, Y. Yoshida, H. Eisaki, T. P. Devereaux, Z. Hussain, Z.-X. Shen, *Nature Phys.* **6**, 414 (2010); Rui-Hua He, M. Hashimoto, H. Karapetyan, J. D. Koralek, J. P. Hinton, J. P. Testaud, V. Nathan, Y. Yoshida, Hong Yao, K. Tanaka, W. Meevasana, R. G. Moore, D. H. Lu, S.-K. Mo, M. Ishikado, H. Eisaki, Z. Hussain, T. P. Devereaux, S. A. Kivelson, J. Orenstein, A. Kapitulnik, and Z.-X. Shen, *Science* **331**, 1579 (2011).

¹¹ K. McElroy, D.-H. Lee, J. E. Hoffman, K. M. Lang, J. Lee, E. W. Hudson, H. Eisaki, S. Uchida, and J. C. Davis, *Phys. Rev. Lett.* **94**, 197005 (2005).

¹² M. Le Tacon, A. Sacuto, A. Georges, G. Kotliar, Y. Gallais, D. Colson, and A. Forget, *Nature Phys.* **2**, 537 (2006).

¹³ Pengcheng Dai, H. A. Mook, R. D. Hunt, and F. Doğan, *Phys. Rev. B* **63**, 54525 (2001); H. He, P. Bourges, Y. Sidis, C. Ulrich, L. P. Regnault, S. Pailhs, N. S. Berzigerova, N. N. Kolesnikov, and B. Keimer, *Science* **295**, 1045 (2002).

¹⁴ See, e.g., M. A. Kastner, R. J. Birgeneau, G. Shirane, and Y. Endoh, *Rev. Mod. Phys.* **70**, 897 (1998), and references therein.

¹⁵ Adrian Cho, *Science* **314**, 1072 (2006).

¹⁶ A. J. Millis, *Science* **314**, 1888 (2006).

¹⁷ S. Hüfner, M. A. Hossain, and F. Müller, *Phys. Rev. B* **78**, 014519 (2008).

¹⁸ See, e.g., M. R. Norman, D. Pines, and C. Kallin, *Adv. Phys.* **54**, 715 (2005), and references therein.

¹⁹ Kai-Yu Yang, T. M. Rice, and Fu-Chun Zhang, *Phys. Rev. B* **73**, 174501 (2006).

²⁰ Zlatko Tešanović, *Nature Phys.* **408**, 408 (2008).

²¹ Shiping Feng, *Phys. Rev. B* **68**, 184501 (2003); Shiping Feng, Tianxing Ma, and Huaiming Guo, *Physica C* **436**, 14 (2006).

²² Huaiming Guo and Shiping Feng, *Phys. Lett. A* **361**, 382 (2007); Yu Lan, Jihong Qin, and Shiping Feng, *Phys. Rev. B* **76**, 014533 (2007); Zhi Wang and Shiping Feng, *Phys. Rev. B* **80**, 064510 (2009).

²³ Zhi Wang, Huaiming Guo, and Shiping Feng, *Physica C* **468**, 1078 (2008); Zhi Wang and Shiping Feng, *Phys. Rev. B* **80**, 174507 (2009).

²⁴ Shiping Feng, Zheyu Huang, and Huaisong Zhao, *Physica C* **470**, 1968 (2010); Zheyu Huang, Huaisong Zhao, and Shiping Feng, *Phys. Rev. B* **83**, 144524 (2011).

²⁵ P. W. Anderson, *Science* **235**, 1196 (1987).

²⁶ Shiping Feng, Jihong Qin, and Tianxing Ma, *J. Phys.: Condens. Matter* **16**, 343 (2004).

²⁷ G. M. Eliashberg, *Sov. Phys. JETP* **11**, 696 (1960); D. J. Scalapino, J. R. Schrieffer, and J. W. Wilkins, *Phys. Rev. B* **148**, 263 (1966).

²⁸ Huaiming Guo and Shiping Feng, *Phys. Lett. A* **355**, 473 (2006).

²⁹ Hai-Hu Wen, Gang Mu, Huiqian Luo, Huan Yang, Lei Shan, Cong Ren, Peng Cheng, Jing Yan, and Lei Fang, *Phys. Rev. Lett.* **103**, 067002 (2009).

³⁰ Huaisong Zhao and Shiping Feng, unpublished.